THE JOURNAL OF BIOLOGICAL CHEMISTRY
Vol. 276, No. 19, Issue of May 11, pp. 16279–16288, 2001

Printed in U.S.A.

Rvb1p and Rvb2p Are Essential Components of a Chromatin Remodeling Complex That Regulates Transcription of over 5% of Yeast Genes*

Received for publication, December 20, 2000
Published, JBC Papers in Press, February 5, 2001, DOI 10.1074/jbc.M011523200

Zophonías O. Jónsson‡, Suman K. Dhar‡§, Geeta J. Narlikar¶, Roy Auty‡‖, Nikhil Wagle‡, David Pellman, Richard E. Pratt‡‡, Robert Kingston¶, and Anindya Dutta‡§§**

*From the ‡Department of Pathology, Brigham and Women's Hospital, Harvard Medical School, Boston, Massachusetts 02115, the ¶Department of Genetics, Massachusetts General Hospital, Boston, Massachusetts 02114, the **Department of Pediatric Oncology, The Dana-Farber Cancer Institute, Harvard Medical School, and the ‡‡Department of Medicine, Brigham and Women's Hospital, Harvard Medical School, Boston, Massachusetts 02115*

Eukaryotic Rvb1p and Rvb2p are two highly conserved proteins related to the helicase subset of the AAA+ family of ATPases. Conditional mutants in both genes show rapid changes in the transcription of over 5% of yeast genes, with a similar number of genes being repressed and activated. Both Rvb1p and Rvb2p are required for maintaining the induced state of many inducible promoters. ATP binding and hydrolysis by Rvb1p and Rvb2p is individually essential *in vivo*, and the two proteins are associated with each other in a high molecular weight complex that shows ATP-dependent chromatin remodeling activity *in vitro*. Our findings show that Rvb1p and Rvb2p are essential components of a chromatin remodeling complex and determine genes regulated by the complex.

Differential gene expression is an important means by which unicellular organisms respond to their environment and lies at the heart of cell specialization in multicellular organisms. Recent discoveries have emphasized the complexity of the apparatus that governs transcription in eukaryotic cells (reviewed in Refs. 1 and 2). The eukaryotic RNA polymerase II holoenzyme, responsible for the transcription of protein-encoding genes, is a megadalton complex containing over 50 components. This large complex must access the template genes on chromosomes packed into chromatin, which restricts access to the DNA. Packaging of genes into chromatin represses basal transcription allowing several multisubunit complexes to regulate gene expression by modulating the topology of the constituent nucleosomes in a number of ways. Histone tails can be modified by either phosphorylation or acetylation (3), and these modifications are correlated with increased transcriptional activity. Another mechanism involves ATP-driven molecular machines that destabilize or remodel nucleosomes directly. These chromatin remodeling factors are all large complexes and all include at least one helicase-like subunit with DNA-dependent ATPase activity (4). The prototype chromatin remodeling complex is the yeast Swi/Snf complex (5, 6), but genetic and biochemical studies have revealed a number of other chromatin remodeling complexes. Inspection of the yeast genome reveals at least 17 ORFs[1] with homology to the Swi/Snf helicase-like ATPase subunit (Snf2p) suggesting that chromatin remodeling complexes are numerous and may each be involved in specific cellular pathways (2, 7). Although Snf2p and its homologs, such as Sth1p, a component of the RSC chromatin remodeling complex (8), and the recently described Ino80p (Ari1p) transcription factor (9, 10) all belong to the DEAD/H class of proteins and contain sequence motifs typical of helicases, none of them has been shown to possess intrinsic helicase activity when purified.

The bacterial RuvB protein belongs to the class of hexameric helicases. Hexameric helicases are members of a larger family of proteins known as the AAA+ class Chaperone-like ATPases (11) that all contain a number of sequence motifs, including Walker A (P-loop) and Walker B boxes that represent active sites for ATP (or dNTP) binding and hydrolysis, respectively. The functional unit of most of these enzymes is a circular hexamer. Recent work in structural biology has shed light on how proteins of this class can translate allosteric changes produced upon ATP hydrolysis into circular movement and vice versa (see Refs. 12 and 13). We first identified the human *RVB1* ortholog in a two-hybrid interaction screen with the 14-kDa subunit of the DNA replication and repair factor RPA, and we subsequently identified yeast *RVB1* in data base searches (14). The protein was named RuvBL1 (RuvB-like) because of its similarity to bacterial RuvB. *RVB*2 (RuvBL2) was subsequently identified as a closely related family member present in the yeast genome, with conserved orthologs in human, fly, and worm. The high degree of sequence conservation in the Rvb1p and Rvb2p proteins immediately suggested that they have important functions *in vivo*, and subsequent genetic studies in yeast showed that both genes are essential for mitotic growth (14, 15). *RVB1* and *RVB2* have been independently discovered a number of times, first in rat as interactors of TATA-binding protein (named TIP49a and TIP49b) (15, 16) and later in human cells as components of a large nuclear protein complex (named ECP-51 and ECP-54) (17) and as es-

* This work was supported in part by grants from the Swiss National Fund for Science (to Z. O. J.) and National Institutes of Health Grant CA60499 (to A. D.). The costs of publication of this article were defrayed in part by the payment of page charges. This article must therefore be hereby marked "*advertisement*" in accordance with 18 U.S.C. Section 1734 solely to indicate this fact.

§ Supported by Postdoctoral Fellowship DAMD17-00-1-0166 from the United States Army Medical Research Acquisition Activity.

‖ Supported by a predoctoral fellowship from Howard Hughes Medical Institutes.

§§ To whom correspondence should be addressed: Dept. of Pathology, Brigham and Women's Hospital, Harvard Medical School, 75 Francis St., Boston, MA 02115. E-mail: adutta@rics.bwh.harvard.edu.

[1] The abbreviations used are: ORFs, open reading frames; pol, polymerase; 5-FOA, 5′-fluoro-orotic acid; MALDI-TOF, matrix-assisted laser desorption ionization/time of flight; FACS, fluorescence-activated cell sorter; Ub, ubiquitin; HA, hemagglutinin; AMP-PNP, adenosine 5′-(β,γ-imino)triphosphate; SAGA, Spt-Ada-Gen5-acetyltransferase.

TABLE I
Yeast strains used in this study

W303-1a	*MATa ade2-1 ura3-1 his3-11,15 trp1-1 leu2-3,112 can1-100*
YUBR1	*MATa his3-11 ubr1Δ::HIS3-GAL-UBR1*
YRVB1	*MATa ura3-1 rvb1Δ::URA3-HA-rvb1-td*
YRVB2	*MATa ura3-1 rvb2Δ::URA3-HA-rvb2-td*
YR1UB1	*MATa ura3-1 his3-11 rvb1Δ::URA3-HA-rvb1-td ubr1Δ::HIS3-GAL-UBR1*
YR2UB1	*MATa ura3-1 his3-11 rvb2Δ::URA3-HA-rvb2-td ubr1Δ::HIS3-GAL-UBR1*
YR1U1B1	*MATa ura3-1 trp1-1 his3-11 rvb1Δ::URA3-HA-rvb1-td ubr1Δ::HIS3-GAL-UBR1 bar1Δ::TRP1*
YR2U1B1	*MATa ura3-1 trp1-1 his3-11 rvb2Δ::URA3-HA-rvb2-td ubr1Δ::HIS3-GAL-UBR1 bar1Δ::TRP1*
YRVB1D	*MATa/α ura3-52/ura3-52trp1Δ63/trp1Δ63 leu2Δ1/leu2Δ1 his3Δ200/his3Δ200 lys2Δ202/lys2Δ202 RVB1/rvb1Δ::HIS3*
YRVB2D	*MATa/α ura3-52/ura3-52 trp1Δ63/trp1Δ63 leu2Δ1/leu2Δ1 his3Δ200/his3Δ200 lys2Δ202/lys2Δ202 RVB2/rvb2Δ::HIS3)*
YKG3	*MATα ura3-52 trp1Δ63 leu2Δ1 his3Δ200 lys2Δ202 rvb1Δ::HIS3 [pRS316/RVB1]*
YRA2	*MATα ura3-52 trp1Δ63 leu2Δ1 his3Δ200 lys2Δ202 rvb1Δ::HIS3 [pRS315/RVB1-3Myc])*

sential interactors of β-catenin (named pontin52 and reptin52) (18, 19) or c-Myc (20).

At the outset of this study, little was known about the function of the Rvb proteins, but in light of the findings that they interacted with TATA-binding protein (15, 16) and were components of the large RNA pol II holoenzyme complex (14), a role in transcription was plausible. However, a different role was implied by the activities of the closest homolog with a known function, eubacterial RuvB, which is involved in the movement of Holliday junctions (branched four-way structures that form upon homologous recombination of DNA). The association with RP-A, a protein involved in DNA replication and repair, implied yet a third possible function for Rvb1p and Rvb2p (14).

Recent publications add to the list of activities attributed to Rvbp. Human Rvb1p and Rvb2p were reported to act independently as helicases of opposite polarity (15, 21), although this result has been disputed (22). More recently a study (23) of a temperature-sensitive mutant strain showed the involvement of Rvb2p in the transcriptional regulation of *CLN2* and genes encoding four ribosomal subunits, and a separate study (10) showed that yeast Rvb1p and Rvb2p copurify with the Ino80p ATPase as a complex that has the ability to remodel chromatin *in vitro*. The mammalian Rvb orthologs have been implicated in cell transformation by c-Myc (20), and the human Rvb proteins were also found to associate with the TIP60 histone acetylase complex and to play a role in repair of DNA damage (22). Finally, a recent study found that the respective *Drosophila* homologs act antagonistically in the control of Wingless signaling through β-catenin-mediated transactivation (19).

In this paper, we report a global analysis of yeast genes affected by removal of Rvb1p or Rvb2p. We used targeted degradation of the Rvb proteins in combination with whole genome high density oligonucleotide arrays (24) to characterize the *in vivo* functions of these proteins. We find that Rvb1p and Rvb2p cooperate, directly or indirectly, in transcriptional regulation of over 5% of yeast genes. In addition, we demonstrate that ATP binding and hydrolysis by the Rvb proteins is essential for their function *in vivo* and that both proteins are components of an ATP-dependent chromatin remodeling complex *in vitro*.

EXPERIMENTAL PROCEDURES

Constructs for Generating Temperature-degradable Alleles—Plasmids used to generate the *rvb1-td* and *rvb2-td* alleles were constructed by replacing the CDC28 fragment in pPW66R (25) with polymerase chain reaction-generated fragments from the N termini of *RVB1* or *RVB2*. The plasmid pKL54 (26) used to place the *UBR1* gene under the control of a *GAL1* promoter was a gift from John F. X. Diffley.

Yeast Strains Genetic Methods and Media—Yeast strains used in this study are isogenic with W303-1a (27), except YRVB1D, YRVB2D, YKG3, and YRA2, which were derived from with YSB455 (14) (Table I). Mating, sporulation, and tetrad analyses were performed by standard methods (28). Rich (YPD), synthetic complete (SD), 5′-fluoro-orotic acid (5-FOA), and sporulation media were prepared as described (28). Media and plates for maintenance of *rvb-td* strains contained 0.1 mM $CuSO_4$. For experiments involving galactose induction, glucose in YPD or SD was substituted with 2% raffinose. Subsequent induction was achieved by switching to medium containing 2% raffinose and 2% galactose.

FACS Analysis—Samples of ~10^7 cells were harvested and fixed in 70% ethanol. Propidium iodide staining and analysis was performed as described in Ref. 29.

Northern Analysis of Gene Expression—Samples of 4×10^7 cells were harvested for each time point and flash-frozen on dry ice. Total RNA was isolated by phenol extraction and precipitation with lithium acetate. Yields were quantified by absorbance at 280 nm, and the samples were subsequently diluted to equal concentration. 5 μg of total RNA were loaded onto each lane on formaldehyde gels following standard protocol (30). Probes were generated by random ^{32}P labeling using ORFs obtained from Research Genetics (Huntsville, AL) as template.

Microarray Analysis of Gene Expression—Transcript profiling with the Affymetrix GeneChips was performed using whole genome high density oligonucleotide arrays (24) according to Affymetrix protocol. Briefly, 8 μg of total RNA were reverse-transcribed using a primer consisting of oligo(dT) coupled to a T7 RNA polymerase-binding site. The cDNA was made double-stranded and biotinylated cRNA synthesized using T7 polymerase. Unincorporated nucleotides were removed, and cRNA was quantitated by UV absorbance. For each sample 25 μl of cRNA were randomly sheared to an approximate length of 50 nucleotides and hybridized (16 h) to the Affymetrix GeneChips. External standards were included in each hybridization to control for hybridization efficiency, to test for sensitivity, and to assist in the comparisons between data sets from different experiments. These external standards were cRNA transcribed from cloned bacterial genes (*bio b, bio c, bio d,* and *cre*). The first hybridization was against a Test II Chip, to determine the quality of the cRNA mixture. Hybridized biotinylated cRNA was detected by incubation with phycoerythrin-streptavidin and was quantitated by scanning using the Hewlett-Packard GeneArray laser scanner. Following positive analysis of the Test Chip, the same hybridization mixture was added to the expression chip, and the chips were hybridized, reacted with phycoerythrin-streptavidin, washed, and then incubated with a polyclonal anti-streptavidin antibody coupled to phycoerythrin as an amplification step to aid in the detection of lower abundance transcripts. Following further washing, the expression chips were scanned as above. Analysis of the scanned data was performed using GeneChip software (version 3.3), Microsoft Access and Microsoft Excel.

Analysis of Microarray Data—Affymetrix GeneChip software was used to calculate average difference (AvgDiff) and fold change (FC) values. For the analysis reported in Table II and in Fig. 4, the 0-h time point for each strain was used as base for the 4-h time point calculations. Analysis was limited to chromosomal ORFs, and non- or marginally expressed genes were discarded based on absent/present calls and a cut-off AvgDiff value of 200 across all six chips. Exceptions were made when a gene was present with an AvgDiff value of >1000 for at least one data set. For genes where negative AvgDiff values remained, a factor increasing the lowest number to 5 was added across the arrays. To select genes that are deregulated in the *rvb-td* strains relative to the wild type strain, ratios of the values for the 0- and 4-h time points for each gene were calculated for the three strains and transformed to linearity by applying a base 2 logarithm, and then the $\log_2$ ratios for the wild type strain were subtracted from the corresponding $\log_2$ ratios for the two *rvb-td* strains. A difference in $\log_2$ ratios greater than 1 corresponds to a more than 2-fold difference in response between *rvb-td* and wild type and was set as cut-off for further analysis. Finally we removed ORFs where confidence in the level of expression at base line was low because of excessive variation in AvgDiff values in the three yeast strains at 23 °C as well as non-annotated ORFs and Ty elements. 326 ORFs passed these criteria and were included in the analysis presented in Fig. 4.

TABLE II
Genes most affected by removal of Rvb1p or Rvb2p

ORF name	Name	Function	Corrected fold change difference[a]	
			rvb1	*rvb2*
YIR032C	DAL3	Ureidoglycolate hydrolase	49.4	15.6
YDL038C		Unknown	−27.1	−42
YDL037C		Similar to glucan 1,4-α-glucosidase	−29.4	−38.3
YGR197C	SNG1	Unknown	−0.1	25
YBR296C	PHO89	Na^+/P_i symporter	−5.6	−19.4
YOR348C	PUT4	Proline and γ-aminobutyrate permease	1	−18.6
YGR184C	UBR1	Ubiquitin-protein ligase (under *GAL* promoter)	−0.9	−17.9
YPR194C		Sexual differentiation protein family	−10.5	−15.7
YMR199W	CLN1	G_1/S cyclin	−6.4	−11.8
YGL088W		Similar to *C. paradoxa* ribosomal protein	3.7	11.5
YDR345C	HXT3	Hexose permease	10.9	11.2
YDL079C	MRK1	Protein kinase	−9.2	−5.8
YJL045W		Unknown	1.7	9.2
YLR081W	GAL2	Glucose and galactose permease	−0.1	−9
YNL142W	MEP2	Ammonia permease	8.8	3.5
YPL223C	GRE1	Unknown; induced by osmotic stress	8.4	8.4
YEL071W	DLD3	D-Lactate dehydrogenase	8.3	3.9
YKL217W	JEN1	Lactate transporter	−1	−7.8
YPL057C	SUR1	Suppresses cls2-2 and rvs161	−1.4	−7.7
YGR208W	SER2	Phosphoserine phosphatase	0.5	7.5
YMR105C	PGM2	Phosphoglucomutase	−1.1	−7.4
YDL227C	HO	Homothallic switching endonuclease	−1.3	−7
YNL277W	MET2	Homoserine *O*-acetyltransferase	−3.6	−6.9
YDL039C		Unknown	−3.5	−6.6
YNR044W	AGA1	α-Agglutinin anchor subunit (mating)	6.2	5.4
YBR018C	GAL7	Gal-1-phosphate uridyltransferase	0.1	−6.2
YHR033W		Unknown; similar to Pro1p	−5.9	−5.2
YDR009W	GAL3	Galactokinase	−2.1	−5.8
YBL048W		Unknown	2	5.8
YBR208C	DUR1,2	Urea amidolyase	0.7	−5.8
YNR075W	COS10	Similar to subtelomerically encoded proteins	−1.1	5.7
YFR053C	HXK1	Hexokinase I	−0.7	−5.5
YBR020W	GAL1	Galactokinase	−0.2	−5.4
YOL058W	ARG1	Arginosuccinate synthetase	4.1	5.3
YPR124W	CTR1	Copper transporter	−3.9	−5.3
YJL088W	ARG3	Ornithine carbamoyltransferase	0.6	5.3
YGR108W	CLB1	G_2/M cyclin	−5.1	−5.1
YNR050C	LYS9	Saccharopine dehydrogenase	−5	−4.7

[a] A negative value denotes a fold decrease in transcription compared to the wild type strain and a positive value an increase in transcription at the 4-h time point. For details see "Experimental Procedures."

The "corrected fold change difference" values reported in Table II were calculated based on GeneChip FC values that incorporate corrections for background noise in the experiments. To calculate differences between a pair of FC values we first reversed scaling applied by the GeneChip software to obtain raw expression ratios according to the formula (|FC| − 1)×(FC/|FC|). The corrected fold change difference (FCdiff) was then calculated for a given gene by subtracting the raw expression ratio of the wild type strain from that of the *rvb-td* strain.

For comparison of the effects of *rvb1-td* with *rvb2-td* and to the effects of *swi1/snf2* deletion (Fig. 5), a less stringent approach was used so as to compare our results with those of Sudarsanam *et al.* (31). Only the values obtained at the non-permissive temperature were used. AvgDiff values were calculated using the wild type strain as base. Non- or low expressing genes were removed based on absent calls and AvgDiff values as above, but with a cut-off at 400. Only genes present in both our data set and the swi1/snf2 data set were included, thus leaving 3991 ORFs for comparison.

Immunoprecipitation and Mass Spectrometry—For immunoprecipitation experiments, 2-liter cultures of the strains YRA2 (*RVB1-3Myc*) and YKG3 were grown in YPD at 30 °C to an A_{600} of 1.0. Cells were harvested by centrifugation, washed once with 500 ml of cold distilled H_2O and once with 500 ml of buffer A (25 mM HEPES-KOH, pH 7.6, 2 mM $MgCl_2$, 1 mM sodium bisulfite, 1 mM dithiothreitol, 1 mM phenylmethylsulfonyl fluoride, 0.5 mM EGTA, 0.1 mM EDTA, 0.02% v/v Nonidet P-40, 20% v/v glycerol) with 0.3 M KCl (buffer A0.3). Pellets were resuspended at 2 ml/g in buffer A0.3 with protease inhibitors (2 μg/ml pepstatin A, 2 μg/ml leupeptin, and 5 μg/ml aprotinin) and extracted on dry ice with a coffee grinder. 20,000 units of DNase I were added to 25 ml of lysate followed by incubation for 15 min on ice, 15 min at room temperature, and 1 h of gentle rocking at 4 °C. After ultracentrifugation for 90 min at 36,000 rpm in a Sorval SW41-Ti rotor, the extracts were pre-cleared with 50 μl of protein A-Sepharose beads (Amersham Pharmacia Biotech) at 4 °C with gentle mixing, incubated with 75 μl of α-Myc (9E10) antibody-coupled protein A-Sepharose beads for 90 min at 4 °C, washed 1× with buffer A with 0.1 M KCl (A0.1), and incubated in 500 μl of A0.1 with protease inhibitors and 1000 units of DNase I for 45 min at 22 °C. Beads were then washed 3× with buffer A0.3, 2× with A0.5, once in A0.1, and eluted by two sequential 30-min incubations at room temperature in 100 μl of A0.1 with 5 mg/ml Myc peptide (EQKLISEEDL). Proteins were subjected to SDS-polyacrylamide gel electrophoresis and silver staining. Bands were excised, destained in-gel, digested with sequencing grade trypsin (Promega), and analyzed by MALDI-TOF mass spectrometry.

ATPase Assay—Ten-μl reactions were incubated for 30 min at 30 °C in 10 mM HEPES-KOH, pH 7.5, 5 mM $MgCl_2$, 1 mM dithiothreitol, 100 μg/ml bovine serum albumin, and 20 μM [α-^{32}P]ATP (33 Ci/mmol) without or with 250 ng of M13mp18 single-stranded DNA, double-stranded plasmid DNA, or chromatinized linear double-stranded DNA. Rvb1p/Rvb2p complex (~50 ng) or equal volumes of mock immunoprecipitate or buffer were added as indicated. Reactions were quenched by adding 1 μl of 0.5 M EDTA on ice. 2.5 μl of each reaction were separated by TLC on PEI-cellulose in 1 M formic acid with 0.5 M LiCl, and visualized by phosphorimaging. Chromatinized DNA (gift from J. Parvin) was prepared with histones purified from chromatin pellet of BJABS cells by gradient dialysis.

Chromatin Remodeling Assay—End-labeled nucleosomal array 5S-G5E4 (32) (gift from J. L. Workman) was formed as described previously (33, 34). Remodeling was carried out at 30 °C in 60 mM KCl, 7% glycerol, 4 mM $MgCl_2$ ± 2 mM ATP·Mg, 0.02% Nonidet P-40, 10 mM HEPES, pH 7.9, and 10 mM Tris, pH 7.5. Reactions were initiated by addition of 4 μl of end-labeled array to a final volume of 20 μl. The final concentration of array was ~1 nM in mononucleosomes with ~1.5 ng/μl of Rvb complex. At various times, 3-μl aliquots were removed and quenched in 4.5 μl of 2% SDS and 100 mM EDTA. The aliquots were deproteinized using

1 mg/ml proteinase K. Cut and uncut arrays were separated on 1% 1xTBE agarose gel and quantified by phosphorimaging.

RESULTS

Removal of Rvb1p or Rvb2p Leads to Growth Arrest at Various Stages in the Cell Cycle—To determine the functions of Rvb1p and Rbv2p *in vivo*, a modification of the N-degron system for temperature-dependent protein degradation was used (25, 26). Briefly, the chromosomal copies of the *RVB* genes were replaced by a fusion consisting of ubiquitin (Ub), the N terminus of mutant *DHFR* (*DHFR-ts*), an HA epitope, and finally the respective *RVB* gene (Fig. 1*A*). Proteolytic removal of Ub results in a fusion protein with an arginine N terminus. At 23 °C the N-terminal arginine of DHFR-*ts* in not recognized by the polyubiquitination/proteasome pathway (25), but upon shift to the non-permissive temperature (38 °C), the N terminus is exposed, and the protein is targeted for processive degradation. To increase the efficiency of degradation, the *UBR1* gene is placed under control of a *GAL1* promoter and tagged with a Myc epitope to facilitate detection (26). After preinduction of Ubr1 with galactose, cultures were shifted to 38 °C, and the degradation of Rvb proteins was monitored by immunoblotting (Fig. 1*C*). The results show that degradation of Rvb1p and Rvb2p is virtually complete within 2 h of temperature shift. Concurrently, growth of the yeast slows down and eventually stops (Fig. 1*B*).

Because of the interaction with RP-A, and the essential nature of the yeast *RVB* genes, we considered that these proteins might have a unique role in S-phase. The morphology of the cells, however, indicated that loss of Rvb1p or Rvb2p resulted in cells ceasing growth in all stages of the cell cycle (not shown). This was confirmed by FACS analysis of propidium iodide-stained cells (Fig. 1*D*). Thus Rvb1p and Rvb2p do not uniquely affect a metabolic process specific for S-phase. The stage in which the majority of cells arrested was highly dependent on conditions, such as the composition of the growth medium, indicating that growth arrest is not dependent on a single check point. For example, in rich medium the cells accumulated predominantly with a 1C DNA content (corresponding to G_1), whereas in minimal medium the cells accumulated mostly with 2C (corresponding to G_2). Such differential effects of Rvb1p and Rvb2p on the cell cycle, depending on whether growth was in rich or minimal media, were reminiscent of the differential effects on transcription caused by the Swi/Snf chromatin remodeling complex (31).

To determine whether the cell proliferation block was reversible and to monitor the viability of the cells after temporary removal of Rvbp, samples were taken at 2-h intervals and plated at 23 °C on YPD containing 0.1 mM $CuSO_4$. The block is reversible with less than 2-fold loss of cell viability after 8 h following the temperature shift. Although viability was only slightly affected, the *rbv-td* strains showed a considerable lag before growth resumed, resulting in a 24-h delay in the appearance of colonies compared with the RVB^+ strain, and a great deal of variation in colony size (data not shown).

While this work was in progress Lim and co-workers (23) published a study of a temperature-sensitive *rvb2* allele (*tih2-160*). When grown on rich medium the strain showed a rapid but reversible accumulation of G_1 cells upon temperature shift, which the authors attributed to a G_1 arrest. These results are in agreement with our observations, but our additional results on minimal media suggest that Rvb1p and Rvb2p are not uniquely required in G_1.

Rvb1p/Rvb2p Are Required for Transcription of Galactose-induced Promoters—The relative difference in the levels of Myc-Ubr1p following induction in galactose in strains with *rvb1-td* and *rvb2-td* first led us to consider that the *RVB1* and *-2* genes had important roles in transcriptional regulation. Whereas Myc-Ubr1p was highly induced by galactose in the control strain (YUBR1), the loss of Rvb1p and Rvb2p in the *td*

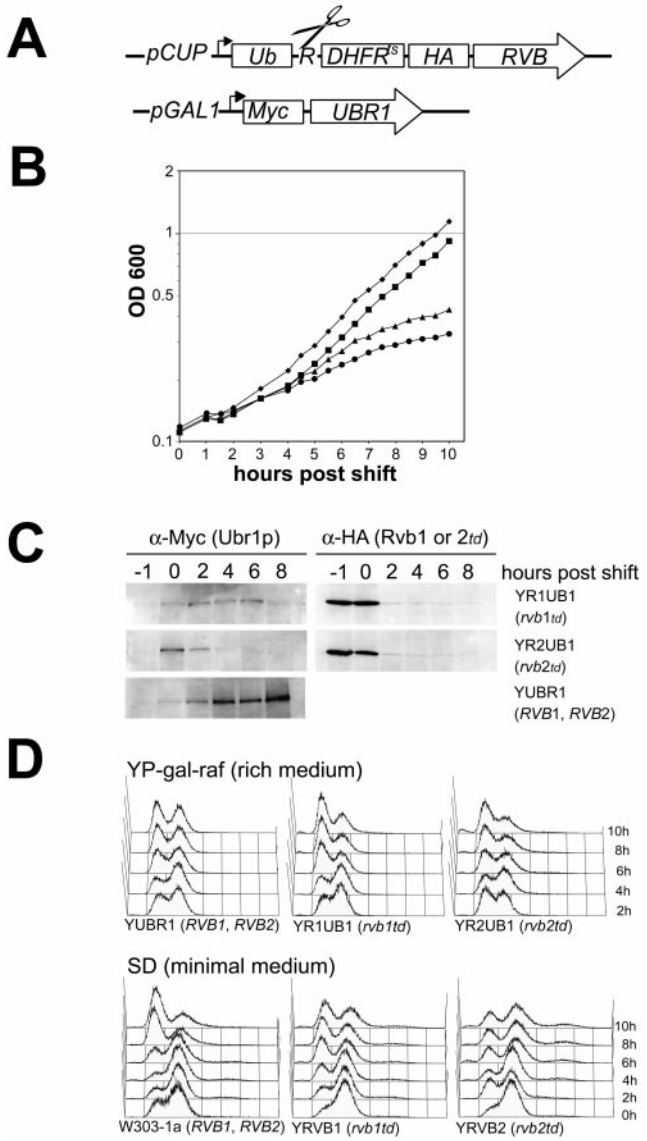

FIG. 1. **Conditional mutants generated by N-degron fusions to Rvb1p and Rvb2p arrest growth under non-permissive conditions.** *A,* a schematic representation of the integrated N-degron constructs and the galactose-inducible *Myc-UBR1*. *B,* cultures of the strains, YUBR1 (■) (W303-1a, *ubr*Δ1::*GAL-Myc-UBR*1), YR1UB1 (▲) (YUBR1, *rvb1*Δ::*DHFR-HA-rvb1-td*), YR2UB1 (●) (YUBR1, *rvb2*Δ::*DHFR-HA-rvb2-td*), and the parent strain W303-1a (♦) were grown to early log phase in YP raffinose at 23 °C. Expression of *UBR*1 from the *GAL1* promoter was induced by adding galactose to 2%. One-hour post-induction the cultures were spun down and transferred to pre-warmed YP containing 2% each, galactose and raffinose. Growth was monitored by measuring A_{600}. Overexpression of Ubr1p does not significantly affect the growth rate, but degradation of either Rvb1p or Rvb2p leads to a gradual cessation of growth. *C,* samples were taken before Gal induction and temperature shift, and at 2-h intervals thereafter. Total protein was extracted as described under "Experimental Procedures," and equal amounts were loaded onto SDS-polyacrylamide gel electrophoresis for Western blotting. Monoclonal α-Myc (9E10) was used to visualize the induction of Myc-Ubr1p, and 12CA5 α-HA antibody was used to monitor the degradation of the HA tagged *rvb-td* proteins. Both Rvb-td proteins are effectively removed within 2 h. *D, rvb-td* mutants do not arrest at a single point in the cell cycle, but cease growth gradually depending on growth conditions. Rapid degradation of Rvb1p or Rvb2p with concurrent Ubr1p overexpression in rich medium leads to accumulation in G_1, whereas strains with endogenous Ubr1 levels grown on minimal medium accumulate with 2C DNA content.

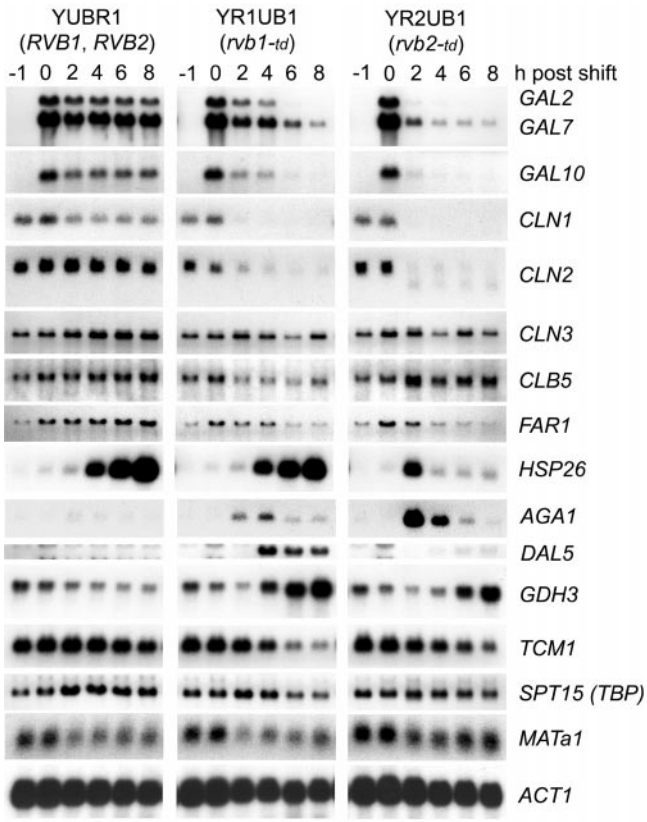

FIG. 2. **RVB1 and RVB2 regulate the expression of a number of genes from different cellular pathways.** Yeast were grown as described in Fig. 1, and samples were taken before addition of galactose (−1 h) and before and after temperature shift. Total RNA was isolated and mRNA levels probed by Northern analysis. The mRNA levels of several genes are strongly affected as discussed in the text.

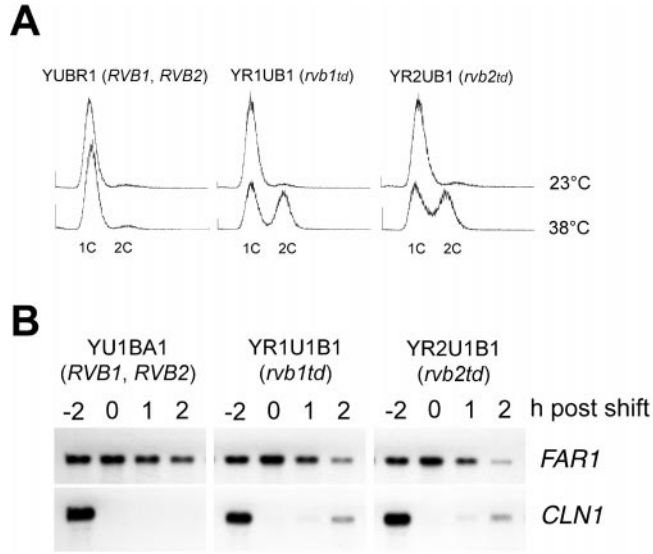

FIG. 3. ***rvb-td* mutants escape prematurely from α-factor block.** *A,* strains were grown at 23 °C in minimal medium containing 2% raffinose, to an A_{600} of 0.1. α-Factor was added to a final concentration of 6 μM and incubated for 1 h; galactose was then added to 2% and incubation continued at 23 °C for 1 h. Additional 6 μM of α-factor was added and incubation continued at room temperature for 1 h by which time shmoos exceeded 80%. The cultures were then split and incubated at either 23 or 38 °C for an additional hour. Samples of the cultures were fixed in 80% ethanol, stained with propidium iodide, and analyzed by FACS. *B,* escape from α-factor block is reflected by changes in the expression of α-factor-regulated genes. After deletion of *BAR1* strains were grown as above. 3 h prior to temperature shift galactose was added to 2%. 1 h later samples were taken (−2 h) for RNA isolation and FACS analysis, and α-factor was added to a final concentration of 0.1 μM. At the 0-h time point samples were taken, the cultures were shifted to the non-permissive temperature of 38 °C, and α-factor was replenished. Changes in expression were followed for 2 h after temperature shift. The figure shows a reduction in transcription of *FAR1* and an increase in *CLN1* levels that reflects the transient release of α-factor block.

strains (YR1UB1 or YR2UB1) was accompanied by a progressive decrease in the amount of Myc-Ubr1 protein (Fig. 1*C*) which was concomitant with the disappearance of *UBR1* mRNA (not shown), consistent with *RVB1* and *RVB2* being required for induction of the *GAL1* promoter that drives *Myc-UBR1*. To test whether this was true for other galactose-responsive promoters, Northern blotting was performed with samples taken at various time points following a temperature shift in the presence of galactose (Fig. 2). The transcripts from several galactose-inducible promoters (*GAL2*, *GAL7*, and *GAL10*) were significantly decreased upon the removal of Rvb1p and Rvb2p from yeast *in vivo*. It is interesting to note that even after activation of the galactose-induced promoter (*0-h lane*), the induced expression is not maintained once Rvb1p or Rvb2p is degraded. This could indicate that the proteins are needed to maintain transcription even after the establishment of a transcriptionally active initiation complex.

Northern Analysis Reveals that the Transcriptional Regulation of a Large Number of Promoters Depends on Rvb1p and Rvb2p—The strong effect of Rvb1p and Rvb2p on the galactose-induced promoters prompted us to examine the effects of *rvb-td* on the levels of several other transcripts after temperature shift. Expression of two G_1 cyclins, *CLN1* and *CLN2* (Fig. 2), was strongly decreased upon loss of Rvb1p or Rvb2p, but the persistence of another G_1 cyclin, *CLN3*, is sufficient to allow cells to progress through G_1. In addition, induction of some heat shock-induced genes (*e.g. HSP26*) was lost upon the removal of Rvb1p or -2p (Fig. 2). However, the expression of *CLB5*, *SPT15*, *MATa1,* and *ACT1* was not significantly affected by temperature shift in the *rvb*1-*td* and *rvb*2-*td* strains (Fig. 2). Thus Rvb1p or Rvb2p are required to regulate the expression of some but not all RNA pol II-transcribed genes.

The rapid changes in gene expression closely follow the degradation of Rvb1p and Rvb2p proteins (Fig. 1*C*) and precede noticeable changes in cell proliferation (Fig. 1*B*). For the most rapidly responsive genes (*e.g. GAL2* and *GAL10*) the transcripts are more than 50% reduced within 1 h of heat shock and almost completely absent after 2 h in the *rvb2-td* strain (Fig. 2 and data not shown). The absence of a lag time is similar to the rapid effect on transcripts seen upon inactivation of RNA pol II core in *rpb1-1* mutants (35), strongly suggesting that the decrease in *GAL* transcripts is a primary effect of Rvb inactivation and not due to general effects of cellular toxicity or growth arrest. Interestingly, several transcripts were up-regulated to different degrees in the absence of either Rvb1p or Rvb2p (*AGA1*, *DAL5*, and *GDH3*), which contrasts with what is seen in temperature-sensitive mutants of RNA pol II or TFIID components.

rvb-td Mutants Escape from α-Factor-induced Cell Cycle Block Due to Defects in Transcriptional Regulation—Experiments designed to examine whether the Rvb1p and Rvb2p were required in S-phase provided further evidence that the proteins were involved in transcriptional regulation. The α-factor mating pheromone was used to arrest cells in G_1 with the aim of releasing the cells into S-phase after inactivation of the Rvbp by temperature shift (Fig. 3). Ubr1p was concurrently induced by addition of galactose. At 23 °C all three strains remained arrested in G_1 by α-factor, but in contrast to the YUBR1 strain (*RVB1* and *RVB2*), a significant proportion of cells in both *rvb1-td* or *rvb2-td* strains escaped from α-factor block when shifted to 38 °C (Fig. 3*A*). Subsequent removal of α-factor did

not cause further cell cycle progression in the *rvb1-td* or *rvb2-td* strains at the non-permissive temperature (data not shown) indicating that the promotion of cell cycle progression was transient. Loss of either Rvb1p or Rvb2p eventually inhibited entry into S-phase and completion of mitosis. The loss of α-factor arrest did not adversely affect mating, since both strains mated as well as wild type, at both 23 and 37 °C in plate mating assays.

Since the induction and maintenance of a G_1 block by pheromone depends on a strict transcriptional program, we reasoned that this program was deregulated by the loss of either Rvb1p or Rvb2p. The secreted Bar1p protease is responsible for degradation of α-factor. Deletion of *BAR1* in the *rvb-td* strains delayed the escape from α-factor block and reduced the number of cells entering S-phase, probably due to a higher effective concentration of α-factor leading to a stronger pheromone response, but did not abolish the effect (Fig. 3*B*). Since α-factor-mediated arrest of the cell cycle depends both on the induction of the Cdc28p inhibitor *FAR1* and repression of G_1 cyclins *CLN1* and *CLN2*, we monitored the responsiveness of these promoters to loss of Rvb1p or Rvb2p. Northern analysis of the α-factor-treated *bar1*Δ, *rvb1-td,* or *rvb2-td* strains revealed that *FAR1* is down-regulated by Rvb removal, whereas the G_1 cyclin *CLN1* is up-regulated (Fig. 3*B*). We conclude that the escape from pheromone-induced block is due to additive changes in the pheromone-specific transcription program, which are reflected by the ratio of cell cycle inhibitor (Far1p) to cell cycle activator (Cln1p) being effectively decreased upon loss of Rvb.

In contrast to the increase in *CLN1* transcript upon temperature shift of *rvb1-td* or *rvb2-td* in the presence of pheromone, similar temperature shift in the absence of pheromone resulted in down-regulation of *CLN1* transcript (Fig. 2). Such opposite effects on the same promoter strongly suggest Rvb1p and Rvb2p are not conventional positive or negative transcription factors but have a more complex function.

Genome Wide Microarray Analysis Reveals That Transcription of Over 5% of Yeast Genes Is Affected in the Absence of Rvb1p or Rvb2p—To address how widespread the requirement of Rvb1p or Rvb2p in yeast transcription is, a genome-wide analysis of gene expression was undertaken by hybridization of cRNA from control and test strains of yeast to high density oligonucleotide arrays representing the whole yeast genome (Affymetrix). Samples taken at the 0-h time point, before temperature shift, were compared with samples taken 4 h after shift to the non-permissive temperature. The 4-h time point was chosen based on the response time seen by Northern blotting with Gal-responsive genes (Fig. 2) to maximize the chance of detecting changes in gene expression while avoiding potential secondary effects due to the growth arrest. As seen in Fig. 1*B* neither *td* strain had ceased growth at this time point. Fig. 4 presents the 326 genes whose expression levels were most significantly altered 4 h after *rvb* inactivation. In addition transcripts of 113 Ty elements or Ty long terminal repeats were at least 2-fold up-regulated upon temperature shift in either *rvb1-td* or *rvb2-td* strains. Thus the transcription of over 5% of active yeast genes is responsive to changes in Rvb1p or Rvb2p levels. The affected genes did not belong to any particular class or cellular pathway as reflected in Table II which shows genes whose transcription was changed more than 5-fold in the *rvb-td* strains compared with wild type. Results from Northern blotting (Fig. 2) agreed well with those obtained by microarray hybridization.

The effects of inactivation are generally similar in the two *rvb-td* strains. This is best demonstrated by the analysis in Fig. 5*A* where the $\log_2$ ratios of the expression level of a gene in the presence or absence of Rvb2p (*y* axis) is plotted against the ratio in the presence or absence of Rvb1p (*x* axis). The strong positive correlation of the two ratios suggests that the two proteins predominantly work together. The correlation coefficient is similar to that reported when comparing the effect of Swi1p with that of Snf2p, which act together in a complex (31).

As seen in both Northern blots (Fig. 2) and the microarray data (Fig. 4 and 5*A*), removal of Rvb2p has, for the most part, a stronger negative effect on transcription than removal of Rvb1p. This raises the possibility that Rvb1p and Rvb2p may also have functions independent of each other. Similarly in the analysis of global gene transcription in Fig. 5*A*, there are a few genes that are in the upper left of lower right quadrants, demonstrating that at least for some promoters Rvb1p and Rvb2p may act in opposite directions. This could be either due to the proteins acting independently of each other or because of differences in the kinetics of protein degradation in the two *rvb-td* strains leading to different kinetics of transcriptional changes in the two strains.

The ATP-binding Sites of Rvb1p/Rvb2p Are Essential for Viability—Lysine to aspartic acid mutations in the Walker A motif of an ATP-binding protein are known to disrupt its ability to bind ATP, whereas aspartic acid to glycine mutations of the Walker B motif do not affect its ability to bind ATP but prevent its hydrolysis (36). These mutations were introduced into the Walker A or B motifs of the yeast *RVB1* or *RVB2* genes (Fig. 6*A*), and the mutant alleles were shown to be incapable of supporting growth. Since both *RVB1* and *RVB2* are essential, dissection of tetrads with *rvb1*Δ*/RVB2* or *rvb2*Δ*/RVB2* results in two viable spores (RVB^+) and two non-viable spores (*rvb*Δ). Transformation of the diploid yeast with a vector expressing the respective wild type Rvb protein but not with empty vector rescued the lethality of *rvb*Δ (Fig. 6*B*). Plasmids expressing the respective *rvb* with mutations in the Walker A or B motifs also failed to rescue the lethality of *rvb*Δ. To eliminate the possibility that the ATP-binding motifs were required for a function of Rvb proteins unique to meiosis or sporulation, haploid yeast were constructed with chromosomal deletions of either *rvb1* or *rvb2*, supported by the wild type allele on an episome that also carried the *URA3* gene. Neither strain grew on 5-FOA that selects against *URA3*. Transformation with a second plasmid carrying the respective wild type *RVB*, however, allowed growth on 5-FOA (Fig. 6*C*). In contrast, transformation with an empty vector or a vector expressing the respective *rvb* with mutations in the Walker A or Walker B motifs did not support growth on 5-FOA. Therefore, ATP binding and hydrolysis by Rvb1p and Rvb2p are required for their essential functions in normal mitotic cell growth and division.

Rvb1p and Rvb2p Associate in a Chromatin Remodeling Complex—The similar effects on gene expression by Rvb1p and Rvb2p (Fig. 5*A*) led us to ask whether the proteins were associated with each other. To this end a yeast strain with a chromosomal deletion of Rvb1p, complemented by a plasmid carrying Rvb1p with three C-terminal Myc tags, was constructed. Immunoprecipitation of Rvb1p-3Myc co-precipitated another yeast protein whose size corresponded to Rvb2p (Fig. 7*A*). MALDI-TOF mass spectrometry was used to identify unambiguously the band as Rvb2p. When compared with mock immunoprecipitations from an isogenic strain harboring a plasmid with untagged Rvb1p, the Rvb1p-3Myc immunoprecipitates reveal a number of bands that are present in substoichiometric ratios to the predominant Rvb1p-Rvb2p protein complex. By analogy to the hexameric helicases, Rvb1p and Rvb2p could form a hetero-hexamer or a hetero-dodecamer, and the presence of lesser amounts of interacting proteins could therefore indicate that they form the core of a larger complex. We attempted to identify these interacting proteins

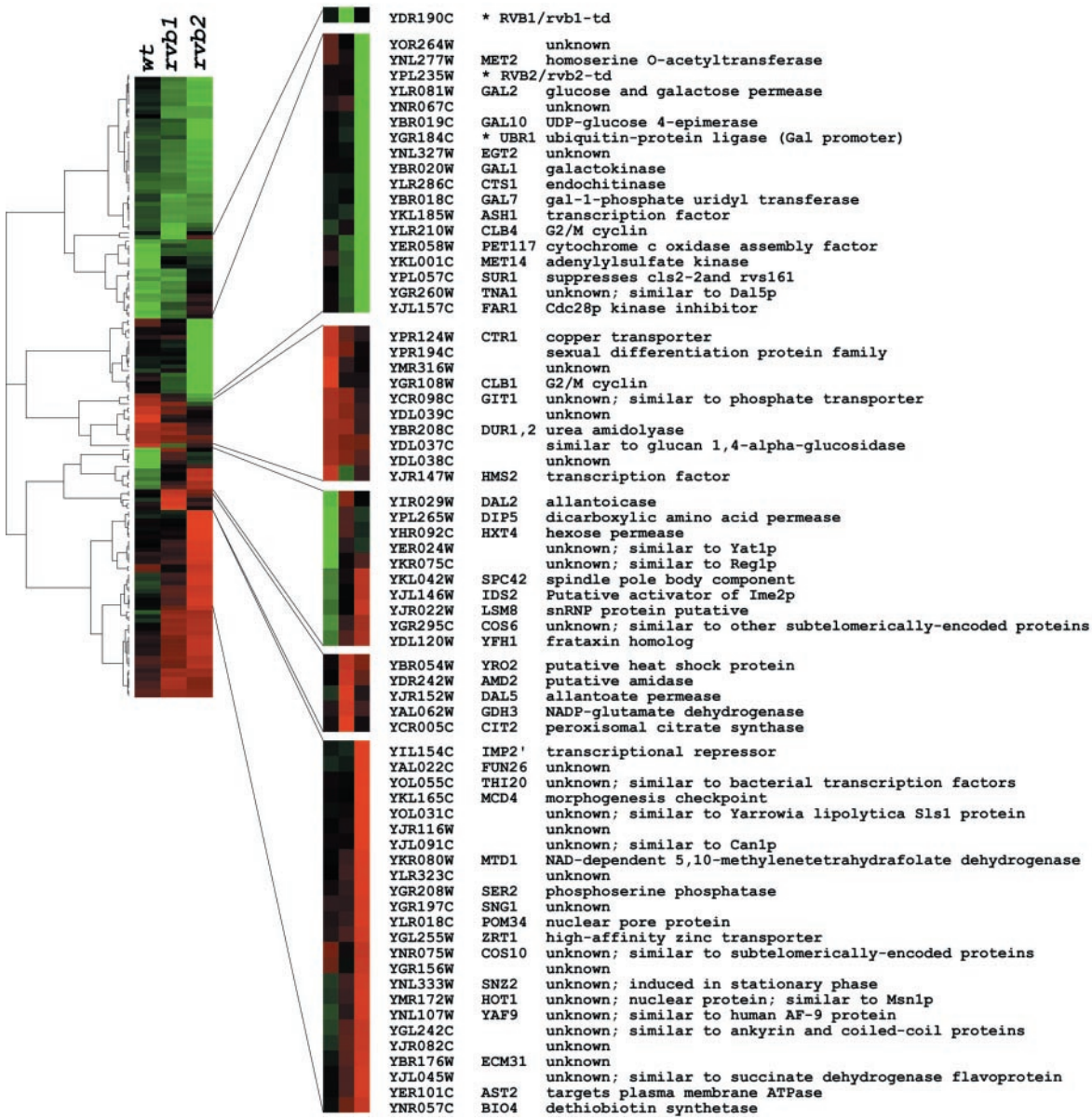

FIG. 4. **Whole genome microarrays (Affymetrix) were used to assess the genome-wide effects of Rvb inactivation.** 8 μg of total RNA were used as substrate as described under "Experimental Procedures." Samples of the three strains, YUBR1, YR1UB1, and YR2UB1, taken before shift to the non-permissive temperature were compared with samples taken 4 h post-shift. Only a subset of ORFs that passed a series of stringent criteria (sufficient abundance and low variation at the permissive temperature) were analyzed as described under "Experimental Procedures." Mitochondrial genes, tRNA genes, and Ty elements were excluded from the analysis. Average Difference values calculated by the GeneChip software (version 3.3) give an estimate of the relative abundance of each transcript. A $\log_2$ ratio was calculated for each ORF for 25/38 °C. The figure shows the $\log_2$ ratios for the 326 genes that were deemed to have a significantly different response to temperature shift in the wild type and mutant strains. The data were clustered with the Cluster software (version 2.11) and visualized by TreeView (version 1.50, Stanford University). *Green* indicates a decrease, and *red* indicates an increase in mRNA abundance. The changes for each gene have been normalized, so the colors indicate relative changes in gene expression in the three strains but are not absolute values.

by excising them from silver-stained gels and performing MALDI-TOF mass spectrometry on their tryptic digests. Only two bands could be unambiguously identified as Actin (Act1p) and the actin-related protein Arp4 (Fig. 7*A*). Interestingly, β-actin is found in the mammalian BAF chromatin remodeling complex (37), and both Act1p and Arp4p are components of the yeast NuA4 histone acetyltransferase complex (22).

The immunoprecipitated Rvb1p-Rvb2p complex was tested for biochemical activities consistent with the suggested role in chromatin remodeling. The complex revealed weak ATPase activity that was slightly stimulated by double- or single-stranded DNA and strongly stimulated by chromatinized DNA (Fig. 7*B*). Helicase assays, utilizing labeled oligonucleotides hybridized to circular M13 DNA failed to detect helicase activity in the complex (data not shown). Finally we assayed the ability of the Rvp1p-Rvb2p complex to remodel chromatin using a linear array of 12 nucleosomes as template. The two central nucleosomes contained 5 Gal4-binding sites, the E4 promoter, and several unique sites recognized by restriction enzymes. These are flanked on either side by 5 nucleosomes positioned via the 5 S ribosomal gene nucleosome positioning sequence. For the remodeling assay, cleavage at the *Hha*I site within one of the central nucleosomes was monitored. As shown in Fig. 7, *C* and *D*, the Rvb complex strongly stimulates cleavage by *Hha*I in the presence of ATP but not in its absence or in the presence of the non-hydrolyzable analog AMP-PNP. No chromatin remodeling activity was seen with equal amounts of the mock immunoprecipitated extract. The level of stimulation

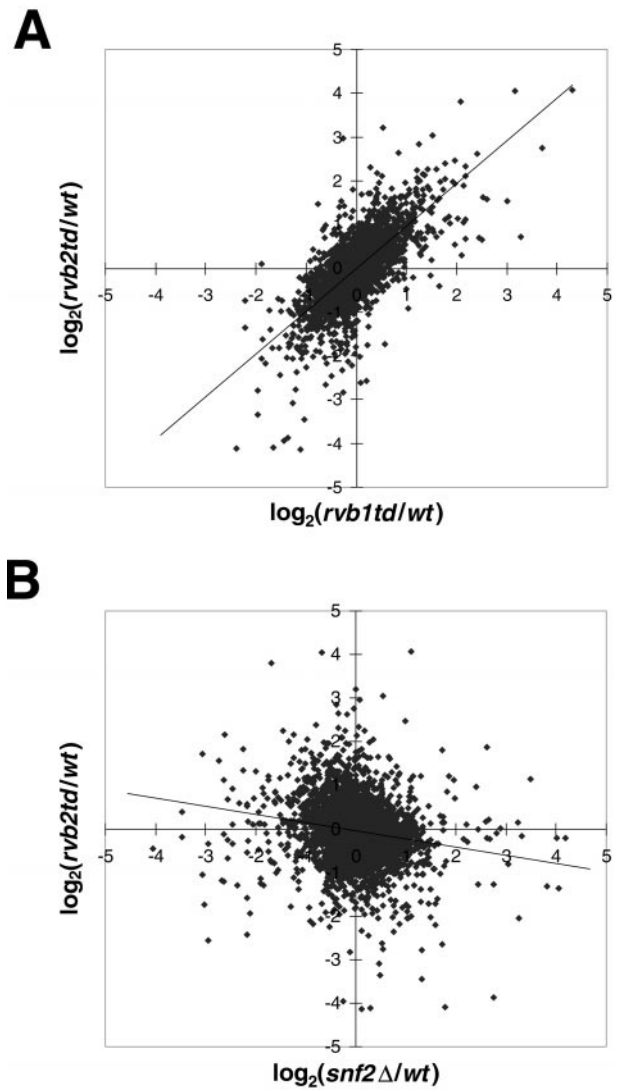

FIG. 5. **Rvb1p and Rvb2p are required for transcription of the same genes *in vivo* but regulate a set of genes different from Swi/Snf.** *A,* the scatter plot portrays the difference in expression of genes in YR1UB1 (*rvb1-td*) and YR2UB1 (*rvb2-td*) relative to the wild type (YUBR1) strain. The transcription ratios in mutant *versus* wild type, after 4 h at the non-permissive temperature, were transformed to linearity by applying a base 2 logarithm such that a 2-fold increase in gene expression in a mutant would equal 1, and −1 corresponded to a 2-fold decrease. A strong correlation ($R^2 = 0.52$) similar to what has been reported for *swi1* and *snf2* ($R^2 = 0.54$) (31) exists between changes in the two strains. *B,* the changes caused by degradation of Rvb2p *versus* the changes in gene expression in the absence of Snf2 show a lack of correlation between the genes affected. For details see under "Experimental Procedures." Note that points can be found far off center in all four quadrants of the graph, reflecting that transcription can be strongly affected in both the same and opposite directions by the two complexes.

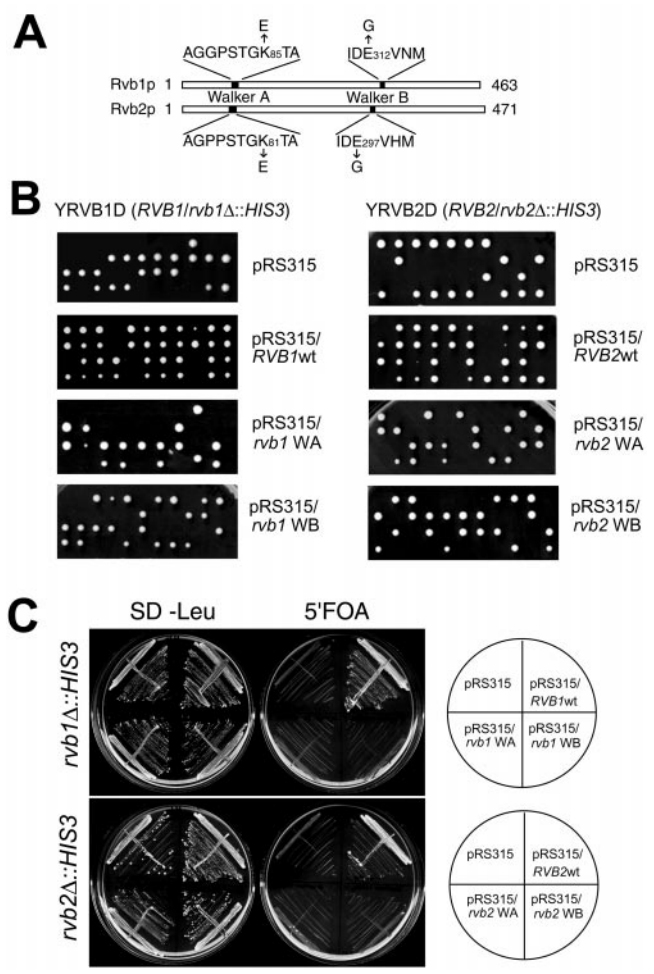

FIG. 6. **ATP binding and hydrolysis by Rvb1p and Rvb2p are independently essential.** *A,* schematic representation of the Walker A and B motifs in Rvb1p and -2p. The mutations indicated were introduced into both motifs in both proteins by site-directed mutagenesis. *B,* Walker motifs in Rvb1p and 2p are individually essential for viability. None of the mutant alleles could substitute for wild type *RVB1* or *-2*. The figure shows tetrad dissection of diploid strains, heterozygous for *rvb1*Δ::*HIS*3 (YRVB1D) or *rvb2*Δ::*HIS*3 (YRVB2D), transformed with either an empty pRS315 or constructs expressing the respective wild type *RVB* or *rvb* mutants from the endogenous promoters. *C,* haploid strains, homozygous for the *rvb* deletions complemented by the wild type alleles on *URA3* expressing plasmids, were used to verify the results. The Walker A and B mutants did not support growth on medium containing 5-FOA.

by the Rvb complex is similar to that seen with the Swi2/Snf1 complex *in vitro* (data not shown). Taken together these results show that Rvb1p and Rvb2p are key components of a complex that has highly specific chromatin remodeling activity *in vitro*. As discussed below, these results are in agreement with the recently published results of Shen *et al.* (10).

Rvb1p/Rvb2p and Swi/Snf Act on Different Sets of Promoters—Given the general similarities between the effects that Rvb proteins and the Swi/Snf chromatin remodeling complex have on transcription, we asked whether the two complexes act on the same or different sets of promoters (Fig. 5*B*). We combined our data with data obtained from Sudarsanam *et al.* (31), which used a similar experimental design to study the effects of deletions of *swi1* or *snf2*. The ratio of transcription levels in the presence or absence of Rvb2p (*y* axis) was plotted against the corresponding ratio in the presence or absence of Snf2p. The lack of correlation between the two ratios is in marked contrast to what was seen with Rvb1p and Rvb2p (Fig. 5*A*) or with Swi1 and Snf2 (31). This analysis suggests that the two chromatin remodeling complexes act independent of each other.

Transcription in many Ty transposon elements was activated upon temperature shift in the *rvb1-td* and *rvb2-td* strains, indicating that Rvb1p and Rvb2p are required for repressing these promoters. Most interesting, the opposite effect, a decrease in Ty element transcription, is seen by disruption of components of the SAGA acetyltransferase complex (38). Further comparison of our data with the data obtained in that study for $TAF_{II}145$ (a component of TFIID), SPT3, SPT20, or GCN5 (components of SAGA) did not reveal further correlation with the genes affected by *rvb1-td or rvb2-td* (not shown). A notable distinction is the predominantly negative effects on transcription caused by mutations in TFIID or SAGA compo-

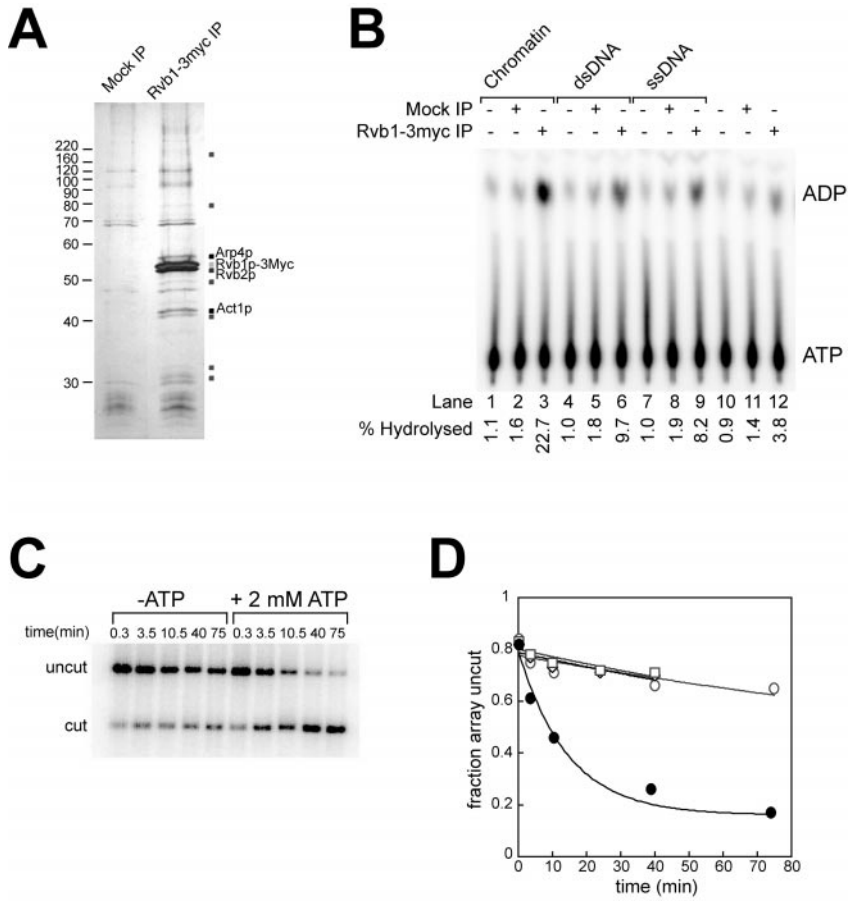

FIG. 7. **Yeast Rvb1p and Rvb2p associate in a complex with ATPase and chromatin remodeling activities.** *A,* immunoprecipitation of Rvb1p and Rvb2p. Indicated bands (*squares*) were excised from the silver-stained gel, digested, and analyzed by MALDI-TOF mass spectrometry. MS-Fit was used to identify Rvb1p from 14 unique peptides (M_r = 1044.55, 1215.67, 1248.63, 1260.65, 1333.69, 1410.81, 1416.75, 1487.70, 1651.93, 1904.04, 1915.96, 1922.00, 1988.06, and 2234.15), Rvb2p from 10 unique peptides (M_r = 1035.53, 1167.63, 1301.66, 1331.72, 1356.57, 1489.75, 1724.87, 1918.03, 2046.12, and 2241.17), Act1p from 4 unique peptides (M_r = 975.44, 1117.50, 1197.70, and 1789.88), and Arp4p from 6 peptides (M_r = 892.42, 914.41, 1108.50, 1114.50, 1139.63, and 1245.67). *B,* the Rvb complex has chromatin-stimulated ATPase activity. Reactions were carried out in the absence or presence of 250 ng of either chromatinized linear double-stranded DNA, circular double-stranded DNA, or single-stranded DNA, followed by separation of products by TLC. *C,* chromatin remodeling assay. PhosphorImager scan of an assay monitoring the digestion of a 12-nucleosome DNA array by *Hha*I in the absence or presence of ATP. The reactions contained end-labeled array template at a concentration of ~1 nM in mononucleosomes and ~30 ng of Rvb1p/Rvb2p complex. *D,* quantitation of PhosphorImager scans shows strong ATP-dependent chromatin remodeling activity in the Rvb complex. ●, Rvb complex + ATP; ○, Rvb complex − ATP; □, Rvb complex + AMP-PNP; and ◇, mock IP + ATP. *IP,* immunoprecipitation.

nents compared with the relatively equal up- and down-regulation seen in *swi*Δ/*snf*Δ and *rvb1-td*/*rvb2-td*.

DISCUSSION

Rvb1p and Rvb2p have widespread and complex effects on gene expression in yeast as shown by the transcriptional up- or down-regulation of hundreds of genes in the *rvb1-td* and *rvb2-td* mutants. As a consequence several essential cellular pathways are interrupted which explains why mitotic growth predominantly ceases in different stages of the cell cycle, depending on conditions. Another example of the general effects caused by Rvb1p and Rvb2p removal is a loss of response to mating factor α, which causes cells to progress to S-phase, although they are unable to complete the cell cycle.

The selective list of promoters that are affected by the loss of Rvb1p or Rvb2p, together with the demonstrated *in vitro* chromatin remodeling activity, suggest that Rvb1p and Rvb2p affect gene expression *in vivo* as components of an ATP-driven chromatin remodeling complex. The fact that many genes are up-regulated in the absence of Rvb1p or Rvb2p makes it unlikely that these are structural elements in the general transcription machinery. A function of Rvbp as a chromatin remodeling factor is consistent with previous reports that a portion of mammalian Rvb1p (RuvBL1) is part of the RNA pol II holoenzyme complex (14) or is associated with TATA-binding protein (16). This result is also consistent with the suggestion that the portion of the *myc* oncogene that interacts with Rvbp is also involved in transcriptional repression, cell transformation, and interaction with TRAAP (also known as PAF400), a 400-kDa protein believed to act in a complex with chromatin-modifying factors (20).

The decreased levels of *GAL2*, *GAL7,* and *GAL10* mRNAs indicate that even after these genes have been induced with galactose, removal of Rvb1p and Rvb2p results in a rapid decrease in transcription. This suggests that Rvb1p and Rvb2p are required after the establishment of a transcriptionally active complex at these promoters. Similarly, the *HSP26* gene was induced following the temperature shift, but an induced state was not maintained when Rvb2p was removed. These results imply that the Rvb1p/Rvb2p-containing complex is required to maintain a state of active transcription. It is interesting that the Swi/Snf complex has also been reported to be required for continuous transcription from some promoters (39), further highlighting the similarities between the two chromatin remodeling complexes.

We also present a comparison of the activities of two chromatin remodeling factors on a genome wide level. Although the Swi/Snf complex and the Rvb1p/Rvb2p-containing complex regulate independent subsets of promoters, transcription of some genes appears to be regulated by both complexes (*e.g. HO* and *GAL1*). This could signify that more than one chromatin remodeling factor could act at a given promoter, either simultaneously or in succession.

Our results agree with the recently published finding that the Snf2p homolog Ino80p can be isolated in a complex with Rvb1p and Rvb2p and a number of other proteins, including Act1p and Arp4p (10). The immunoprecipitated Ino80 complex increased the accessibility of a chromatinized DNA template to restriction endonuclease. The authors compared the Ino80p complex with an immunoprecipitate of FLAG-tagged Rvb2p which yielded a complex with a composition that appears nearly identical to our Rvb1p-3Myc complex, although we cannot unambiguously identify the ~175-kDa Ino80 subunit in the Rvb1–3Myc immunoprecipitated complex. Other differences between the Ino80 complex used in their study and our Rvbp

complex are reflected in the relative abundance of the various bands and the presence of a few bands that are specific to the Rvbp complex. The low amounts of Ino80 in the Rvbp complex could explain the relatively weak ATPase activity and apparent lack of helicase activity in our preparations compared with what is reported for the Ino80 complex. However, the chromatin remodeling activity in the Rvbp complex is remarkably strong, suggesting that Rvb1p/Rvb2p may contain the active chromatin remodeling activity or that some of the unidentified subunits of the complex may substitute for Ino80p. Accordingly, *ino80* null mutants are viable but show decreased expression of a number of genes such as *PHO5*, *GAL1*, *CYC1,* and *ICL1* (9), whereas *rvb* null mutations are lethal.

Another recent study of the 14-subunit TIP60 histone acetylase complex from human cells revealed the presence of both Rvb orthologs in the complex along with β-actin and the actin-related protein BAF53 (22). These results suggest that the mammalian Rvb1p/Rvb2p orthologs may have an alternative chromatin remodeling function through interaction with histone acetylase. The Esa1p acetylase of yeast is a homolog of TIP60 and is associated with Tra1p, Act1p, and Arp4p in the NuA4 complex. Tra1p is a homolog of PAF400, which is a component of the TIP60 complex. Similarly Act1 and Arp4p are homologs of β-actin and BAF53, respectively, implying that NuA4 and TIP60 have similar functions. We could not, however, detect the presence of HA-tagged Esa1p in Rvb1p immunoprecipitates,[2] and others have failed to detect Rvb subunits in yeast NuA4 (22). This suggests differences in the structural composition of Rvb1p-Rvb2p complex in yeast and mammalian cells.

The precise function of the Rvb proteins in transcription in yeast and human cells awaits further study, but the results presented here show that both proteins are transcriptional regulators that form a complex with chromatin remodeling activities. Further genetic and biochemical analyses of Rvb1 and Rvb2 will help us understand the mechanisms by which they act, as well as their roles in controlling transcription *in vivo* and their possible contribution to the pathogenesis of human malignancies.

Acknowledgments—We thank James Wohlschlegel for assistance with MALDI-TOF spectrometry; Neelima Mondal and Jeffrey Parvin for chromatinized plasmid DNA and critical discussions, and Nicole Francis for providing the assembled array template.

REFERENCES

1. Perez-Martin, J. (1999) *FEMS Microbiol. Rev.* **23,** 503–523
2. Muchardt, C., and Yaniv, M. (1999) *J. Mol. Biol.* **293,** 187–198
3. Luger, K., and Richmond, T. J. (1998) *Curr. Opin. Genet. & Dev.* **8,** 140–146
4. Eisen, J. A., Sweder, K. S., and Hanawalt, P. C. (1995) *Nucleic Acids Res.* **23,** 2715–2723
5. Cairns, B. R., Kim, Y. J., Sayre, M. H., Laurent, B. C., and Kornberg, R. D. (1994) *Proc. Natl. Acad. Sci. U. S. A.* **91,** 1950–1954
6. Cote, J., Quinn, J., Workman, J. L., and Peterson, C. L. (1994) *Science* **265,** 53–60
7. Cherwitz, S. A., Aravind, L., Sherlock, G., Ball, C. A., Koonin, E. C., Dwight, S. S., Harris, M. A., Dolinski, K., Mohr, S., Smith, T., Weng, S., Cherrz, J. M., and Botstein, D. (1998) *Science* **282,** 2022–2028
8. Du, J., Nasir, I., Benton, B. K., Kladde, M. P., and Laurent, B. C. (1998) *Genetics* **150,** 987–1005
9. Ebbert, R., Birkmann, A., and Schuller, H. J. (1999) *Mol. Microbiol.* **32,** 741–751
10. Shen, X., Mizuguchi, G., Hamiche, A., and Wu, C. (2000) *Nature* **406,** 541–544
11. Neuwald, A. F., Aravind, L., Spouge, J. L., and Koonin, E. V. (1999) *Genome Res.* **9,** 27–43
12. Sawaya, M. R., Guo, S., Tabor, S., Richardson, C. C., and Ellenberger, T. (1999) *Cell* **99,** 167–177
13. Fillingame, R. H. (1999) *Science* **286,** 1687–1688
14. Qiu, X. B., Lin, Y. L., Thome, K. C., Pian, P., Schlegel, B. P., Weremowicz, S., Parvin, J. D., and Dutta, A. (1998) *J. Biol. Chem.* **273,** 27786–27793
15. Kanemaki, M., Kurokawa, Y., Matsu-ura, T., Makino, Y., Masani, A., Okazaki, K., Morishita, T., and Tamura, T. A. (1999) *J. Biol. Chem.* **274,** 22437–22444
16. Kanemaki, M., Makino, Y., Yoshida, T., Kishimoto, T., Koga, A., Yamamoto, K., Yamamoto, M., Moncollin, V., Egly, J. M., Muramatsu, M., and Tamura, T. (1997) *Biochem. Biophys. Res. Commun.* **235,** 64–68
17. Salzer, U., Kubicek, M., and Prohaska, R. (1999) *Biochim. Biophys. Acta* **1446,** 365–370
18. Bauer, A., Huber, O., and Kemler, R. (1998) *Proc. Natl. Acad. Sci. U. S. A.* **95,** 14787–14792
19. Bauer, A., Chauvet, S., Huber, O., Usseglio, F., Rothbacher, U., Aragnol, D., Kemler, R., and Pradel, J. (2000) *EMBO J.* **19,** 6121–6130
20. Wood, M. A., McMahon, S. B., and Cole, M. D. (2000) *Mol. Cell* **5,** 321–330
21. Makino, Y., Kanemaki, M., Kurokawa, Y., Koji, T., and Tamura, T. (1999) *J. Biol. Chem.* **274,** 15329–15335
22. Ikura, T., Ogryzko, V. V., Grigoriev, M., Groisman, R., Wang, J., Horikoshi, M., Scully, R., Qin, J., and Nakatani, Y. (2000) *Cell* **102,** 463–473
23. Lim, C. R., Kimata, Y., Ohdate, H., Kokubo, T., Kikuchi, N., Horigome, T., and Kohno, K. (2000) *J. Biol. Chem.* **275,** 22409–22417
24. Wodicka, L., Dong, H., Mittmann, M., Ho, M. H., and Lockhart, D. J. (1997) *Nat. Biotechnol.* **15,** 1359–1367
25. Dohmen, R. J., Wu, P., and Varshavsky, A. (1994) *Science* **263,** 1273–1276
26. Labib, K., Tercero, J. A., and Diffley, J. F. (2000) *Science* **288,** 1643–1647
27. Thomas, B. J., and Rothstein, R. (1989) *Cell* **56,** 619–630
28. Rose, M. D., Winston, F., and Hieter, P. (1990) *Methods in Yeast Genetics: A Laboratory Manual*, Cold Spring Harbor Laboratory, Cold Spring Harbor, NY
29. Nash, R., Tokiwa, G., Anand, S., Erickson, K., and Futcher, A. B. (1988) *EMBO J.* **7,** 4335–4346
30. Ausubel, F. M., Brent, R., Kingston, R. E., Moore, D. D., Seidman, J. G., Smith, J. A., and Struhl, K. (1987) *Current Protocols in Molecular Biology*, (Nolan, C., and Ferguson, M., eds) pp. 7.37–7.52, Greene Publishing Associates and Wiley-Interscience, New York
31. Sudarsanam, P., Iyer, V. R., Brown, P. O., and Winston, F. (2000) *Proc. Natl. Acad. Sci. U. S. A.* **97,** 3364–3369
32. Neely, K. E., Hassan, A. H., Wallberg, A. E., Steger, D. J., Cairns, B. R., Wright, A. P., and Workman, J. L. (1999) *Mol. Cell* **4,** 649–655
33. Logie, C., and Peterson, C. L. (1997) *EMBO J.* **16,** 6772–6782
34. Phelan, M. L., Schnitzler, G. R., and Kingston, R. E. (2000) *Mol. Cell. Biol.* **20,** 6380–6389
35. Holstege, F. C., Jennings, E. G., Wyrick, J. J., Lee, T. I., Hengartner, C. J., Green, M. R., Golub, T. R., Lander, E. S., and Young, R. A. (1998) *Cell* **95,** 717–728
36. Perkins, G., and Diffley, J. F. (1998) *Mol. Cell* **2,** 23–32
37. Zhao, K., Wang, W., Rando, O. J., Xue, Y., Swiderek, K., Kuo, A., and Crabtree, G. R. (1998) *Cell* **95,** 625–636
38. Lee, T. I., Causton, H. C., Holstege, F. C., Shen, W. C., Hannett, N., Jennings, E. G., Winston, F., Green, M. R., and Young, R. A. (2000) *Nature* **405,** 701–704
39. Biggar, S. R., and Crabtree, G. R. (1999) *EMBO J.* **18,** 2254–2264

[2] Z. O. Jónsson, R. Auty, and A. Dutta, unpublished observations.

Rvb1p and Rvb2p Are Essential Components of a Chromatin Remodeling Complex That Regulates Transcription of over 5% of Yeast Genes

Zophoni?as O. Jónsson, Suman K. Dhar, Geeta J. Narlikar, Roy Auty, Nikhil Wagle, David Pellman, Richard E. Pratt, Robert Kingston and Anindya Dutta

J. Biol. Chem. 2001, 276:16279-16288.
doi: 10.1074/jbc.M011523200 originally published online February 5, 2001
